RSC Pharmaceutics

ROYAL SOCIETY OF CHEMISTRY

PAPER

View Article Online
View Journal

Cite this: DOI: 10.1039/d6pm00077k

A dual cross-linked biodegradable polyelectrolyte hydrogel actuator for bi-directional pH-responsive drug release

Govind Choudhary,[a] Soni Jadoun,[a] Komal Rani,[a] Manikrishna Lakavathu[b] and Aashish Sharma *[a]

Here, we present a dual cross-linked pH-responsive hydrogel platform for controlled drug release in acidic and basic pathophysiological pH media. The hydrogel was strategically developed using oppositely charged polyelectrolytes, namely gelatin and carboxymethyl cellulose (CMC). This hydrogel was stabilised by adding a cross-linking agent, 1,4-butanediol diglycidyl ether (BDDE). The hydrogel could be formulated in about 2 h, at pH 9, without any specialised instruments. The prepared hydrogel senses both lower and higher environmental pH and swells to deliver the drug to the intended application site. Importantly, the prepared hydrogel was found to exhibit an equal percentage (~60%) of shrinkage (at pH 7.4) and swelling (at pH 4 and 9). The novelty of the proposed hydrogel lies in its reversible sensitivity to pH for on-demand drug delivery in both acidic environments (*e.g.* tumour sites) and basic environments (*e.g.* chronic wounds). Neomycin sulphate, a common drug effective against chronic wounds and cancer, could be entrapped within the hydrogel with excellent entrapment efficiency (~84%). Entrapped neomycin sulphate is released on demand in acidic (pH ~6) and basic (pH ~9) media. This polyelectrolyte-based hydrogel is bio-degraded within 21 days. Changes in the hydrogel's morphology were observed through SEM. The reported hydrogel exhibits remarkable biocompatibility also for HeLa cell lines. Therefore, this prepared hydrogel may be a promising pH-responsive biomaterial for drug delivery applications, which can easily be scaled up in the future.

Received 27th February 2026,
Accepted 16th April 2026

DOI: 10.1039/d6pm00077k

rsc.li/RSCPharma

1. Introduction

In recent years, hydrogels have drawn the interest of biomaterials scientists as one of the most promising drug delivery technologies for various modes of administration, including topical, parenteral, oral, ocular, vaginal and rectal.[1–3] Because of their exceptionally high water content, hydrogels exhibit excellent biocompatibility, have a morphological resemblance to human tissues, and have a tunable capacity to encapsulate hydrophilic drugs.[3] These encapsulated drugs can be released from hydrogels in response to certain stimuli like pH, temperature, enzymes, certain biomolecules (*e.g.* glucose) and reactive oxygen species.[4–6] These stimulus-responsive hydrogels integrate controlled drug delivery due to their ability to respond to the above-mentioned external stimuli. Such stimulus-responsive hydrogels incorporate various polymers and cross-linkers according to the intended stimuli. Among all the above-mentioned stimuli, tissue-specific pH under healthy and diseased conditions is being explored in detail to develop stimulus-responsive hydrogels for drug delivery applications. For example, the lower pH in the vicinity of cancer cells and the higher pH of chronic wounds as compared to physiological pH have been utilised for drug delivery purposes.[7,8] pH-Responsive hydrogels have also been reported to deliver the drugs under various conditions like those found in peptic ulcers, respiratory diseases, ulcerative colitis, arthritis, bacterial infections, *etc.*[2,9] However, the majority of reported pH-sensitive hydrogels sense either acidic or basic pH only, and hence can deliver the encapsulated drug under the pathological conditions in either an acidic or a basic pH medium. The current exploration endeavoured to resolve this problem by the meticulous selection of ionizable polymers (polyelectrolytes).

To address this problem, we reviewed numerous reports on pH-responsive hydrogels and found that the reported hydrogels incorporate various natural and synthetic polymers bearing pH-dependent cationic charge (cationic polyelectrolytes) and anionic charge (anionic polyelectrolytes).[10,11] Mainly, chitosan,[12,13] gelatin,[14–16] collagen,[17,18] PEI,[19,20] poly(amino) methacrylate/poly(amino) acrylate,[21] poly(β-aminoester),[21] polyurethane,[21] and poly(4-vinylpyridine)[22] are used as cationic poly-

[a]*Department of Pharmacy, School of Healthcare and Allied Sciences, Sohna-Gurugram Road, Sohna-122103, Gurugram, Haryana, India. E-mail: pharma.aashish@gmail.com*
[b]*Indian Institute of Science Education and Research Thiruvananthapuram (IISER TVM), Maruthamala, PO, Vithura, Thiruvananthapuram-695551, Kerala, India*

electrolytes, while alginic acid,[9,23] hyaluronic acid,[24,25] chondroitin sulphate,[26] carboxymethyl cellulose,[27,28] carrageenan,[29] polyaspartic acid,[30,31] polyacrylic acid,[32,33] *etc.*, are used as anionic polyelectrolytes to formulate pH-responsive hydrogels. These polyelectrolytes interact through electrostatic interactions to create a 3D hydrogel network, which holds water and can entrap various drugs. These electrostatic interactions are pH dependent; hence, they make the hydrogel unstable beyond a certain pH range. Changing the pH beyond a particular value may neutralise the charge on these polyelectrolytes and allow both of the counter polyelectrolytes to separate from each other. The separation of the neutralised polyelectrolytes of a hydrogel becomes more prominent when hydrogels soak in an aqueous medium. During the process of soaking, the inflow of water molecules into the hydrogels propels the neutralised polyelectrolytes forcefully apart from each other, resulting in swelling of the hydrogels, which in turn makes the hydrogels highly unstable. In this process, the entrapped drug gets released from the hydrogels without any control (*viz.*, burst release).[10]

This uncontrolled drug release results from the complete separation of the neutral polyelectrolytes of the hydrogels. Here, we endeavoured to hinder the separation of neutralised polyelectrolytes to control the burst release by putting suitable covalent cross-links between the counter polyelectrolytes. These covalent cross-links keep hold of the polyelectrolytes even under charge-neutralised conditions during swelling of the hydrogels. These covalent cross-links act as anchors that allow neutralised polyelectrolytes to move upon swelling but prevent complete disruption of the hydrogels to control the drug release as a function of pH.[3]

Researchers have employed various cross-linking chemistries for developing hydrogels, which mainly include Schiff's base,[34–36] disulphide bonds,[37,38] thiol–ene,[39–41] thiol–yne,[41,42] alkyne–azide,[43] thiol–Michael addition,[44] DOPA crosslinks,[45] and enzymatic cross-linking[46–48] to name a few. To employ these cross-linking chemistries, either natural polymers are derivatised with suitable functionalities or entirely new polymers have to be synthesised. Sometimes, functionalization of natural polymers is a prerequisite condition for employing different cross-linking chemistries, which may bring these polymers out of the FDA-approved list. However, incorporating FDA-approved polymers in hydrogels may enhance the chances of commercialisation of such formulations.[49]

Moreover, some of the cross-linking chemistries additionally need external impetus, such as thiol–ene/thiol–yne cross-linking, which requires photo-initiators and UV-light.[39–41] Alkyne–azide cross-links need a copper-based catalyst,[43] thiol–maleimide chemistry needs a suitable base,[50] and DOPA-based cross-links entail metal ions (Fe^{3+}), periodates or enzymes,[51–53] while enzymatic cross-links unequivocally need suitable enzymes to cross-link the polyelectrolytes.[54,55] Although few reported thiolated polyelectrolytes can form disulphide bonds (thiol-to disulphide conversions) without any external reagent, this has been explored by us in our earlier published reports.[56,57]

Apart from the above-mentioned cross-linkers, there are certain cross-linkers such as glutaraldehyde, 1,4-butanediol diglycidyl ether (BDDE), divinyl sulphone (DVS), *etc.*, which can cross-link the different biopolymers without further functionalization.[58–60] Glutaraldehyde (GTA) (including other dialdehyde analogues), BDDE and DVS can crosslink chitosan,[61–63] gelatin,[58,64,65] and collagen[66–68] through their amine functionalities. Anionic polymers such as hyaluronic acid,[69] carboxymethyl cellulose,[70–72] starch,[73] *etc.*, have also been cross-linked successfully for developing different biomaterial formulations. Most of the researchers have used dialdehydes, BDDE and DVS for cross-linking one type of polymer, either cationic or anionic polyelectrolytes. For example, Faivre *et al.* reviewed and reported the cross-linking of hyaluronic acid by DVS and BDDE.[74] Sala *et al.* developed a hydrogel by cross-linking two anionic polymers, HA and CMC, using BDDE.[71] Similarly, cationic polymers have also been cross-linked to develop hydrogels; for example, Privar and co-workers developed a chitosan hydrogel by using diglycidyl ethers of glycols.[75] On the other hand, some scientists have explored one type of cross-linking only for developing hydrogels, either through primary alcohol (*e.g.* for HA)[74] or through primary amines (*e.g.* for chitosan and gelatin).[76] It is noteworthy that incorporating the same polymer or a similar type of polymer for constructing a biomaterial formulation may limit the inclusion of beneficial features of different polymers in a single formulation. Most of the reported pH-responsive hydrogels have been found to deliver the entrapped drugs in either a basic medium or an acidic medium (*i.e.* unidirectional).[10,77] In the current study, we present a single hydrogel platform to deliver the drugs in both acidic media (*e.g.* in the vicinity of cancer cells)[20] and basic media (*e.g.* in the proximity of chronic wounds).[78]

Here, we report a polyelectrolyte-based bi-directional pH-sensitive hydrogel for controlled drug delivery applications (Fig. 1). The proposed hydrogel is strategically composed of gelatin, a cationic polyelectrolyte which has primary amino groups, carboxymethyl cellulose (CMC), an anionic polyelectrolyte having carboxyl groups, and a cross-linker BDDE, which is equipped with two nucleophile-sensitive epoxy functionalities at the opposite ends of propyloxybutane. The primary amino groups of gelatin not only participate in generating pH-dependent cationic charge but also serve as nucleophilic cross-linking sites to react with the epoxy rings of BDDE without compromising its ability to develop pH-dependent cationic charge (*viz.*, the generation of secondary amines in cross-links). In the case of CMC, carboxyl groups participate to generate pH-dependent anionic charge and contribute as cross-linking sites to react with the epoxy rings of BDDE. All three basic components, gelatin, CMC and BDDE, are USFDA approved for biomaterials and implants and are known for being biodegradable and biocompatible.[79–81] Thus, the significance of the formulated hydrogel lies in the following features: (I) bi-directional pH-responsive behaviour, (II) controlled drug release in acidic and basic media, (III) highly reversible pH-responsiveness, (IV) biodegradability, (V) non-toxicity to mam-

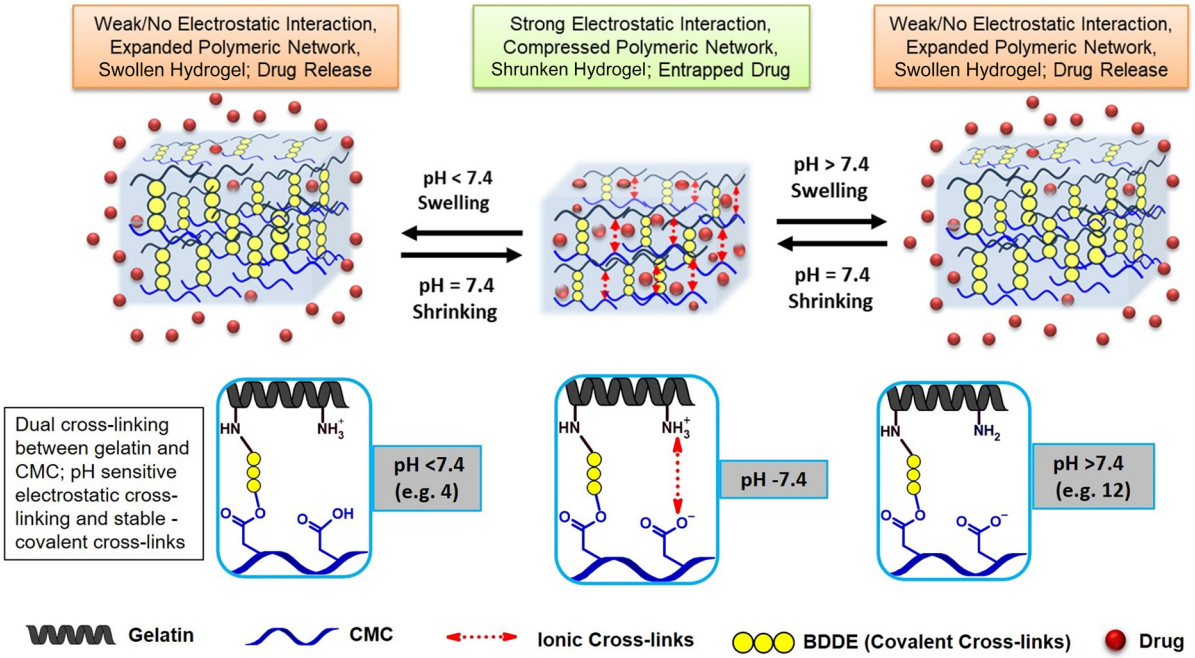

Fig. 1 Showcasing the basic design of a bi-directional pH-sensitive hydrogel, pH-responsive drug release and dual cross-linking between gelatin and CMC.

malian cells, and (VI) an affordable and scalable formulation, an essential criterion for "bench to bedside" translation. The structural and performance details of the hydrogels prepared from these natural polyelectrolytes (NPEs) are presented below.

2. Experimental section

2.1. Materials and methods

Gelatin type A (bloom strength – 250 g) and CMC (avg. mol wt – 20 kDa) were procured from Central Drug House (P) Ltd, New Delhi, India, BDDE was procured from Spectrochem, India, and neomycin sulphate (NEO) was purchased from Yarrow Chem, Mumbai, India. All the UV-visible spectra were recorded using a SHIMADZU UV-1800. Rheological measurements were carried out on a RheoCampass MCR302 rheometer (Anton Paar India Pvt. Ltd). Scanning electron microscopy was performed on a high-resolution field emission scanning electron microscope, JEOL JSM-7610F Plus.

2.2. Formulation and optimisation of hydrogels

20% w/v gelatin solutions (Type A, bloom strength 250 g) in phosphate buffers of three different pH levels (pH 7.4, pH 9 and pH 12) were prepared by heating at 40 °C for 1 h. Similarly, 1% w/v CMC solutions in phosphate buffers of three different pH levels (pH 7.4, pH 9 and pH 12) were prepared at RT. 2 mL of the gelatin solution and 2 mL of CMC solution (20% w/v) were loaded into a double-barrel syringe. The contents were co-injected into a clean vial, ensuring simultaneous mixing of both solutions (Fig. 2). Subsequently, different volumes (20 μL, 40 μL, 60 μL, 80 μL and 100 μL) of 1,4-butanediol diglycidyl ether (BDDE) were added as a crosslinking agent to the polymeric solution at all three pH levels (Table 1). Each of the solutions was stirred continuously for 15 minutes at 40 °C to ensure thorough mixing and initiation of the cross-linking reaction. After mixing, the content was transferred to vials, which were then placed in a water bath to heat the solution to 40 °C. Over time, gelation was observed, indicating the successful formation of a crosslinked hydrogel network between CMC and gelatin *via* BDDE (Fig. 2).

2.3. Confirmation of the gelation-vial inversion test

The gelation times for all the trials of hydrogels were determined by following the earlier published reports[82–84] using the vial inversion method and are provided in Table 1. Predetermined hydrogel solutions (Table 1) were incubated in a glass vial at a controlled temperature of 40 ± 1 °C. The vials were inverted at certain time intervals to examine the flow of the hydrogel solutions by visual examination. The gelation time was identified as the point at which the hydrogel solution stopped flowing.[85] The gelation times of all the hydrogel samples are summarised in Table 1. Among all the hydrogel samples, Gel-III (due to it is having the shortest gelation time) was selected for further studies.

2.4. Swelling/shrinking behaviour of hydrogels

Gel-III hydrogels were cast and cured in a cylindrical shape having a 2 cm diameter and 1 cm height. Swelling was assessed volumetrically by measuring the diameter and height with a scale. Gel-III hydrogels were prepared, and the volume of the prepared hydrogels was recorded. Gel-III hydrogels were then placed separately in different beakers containing 10 mL

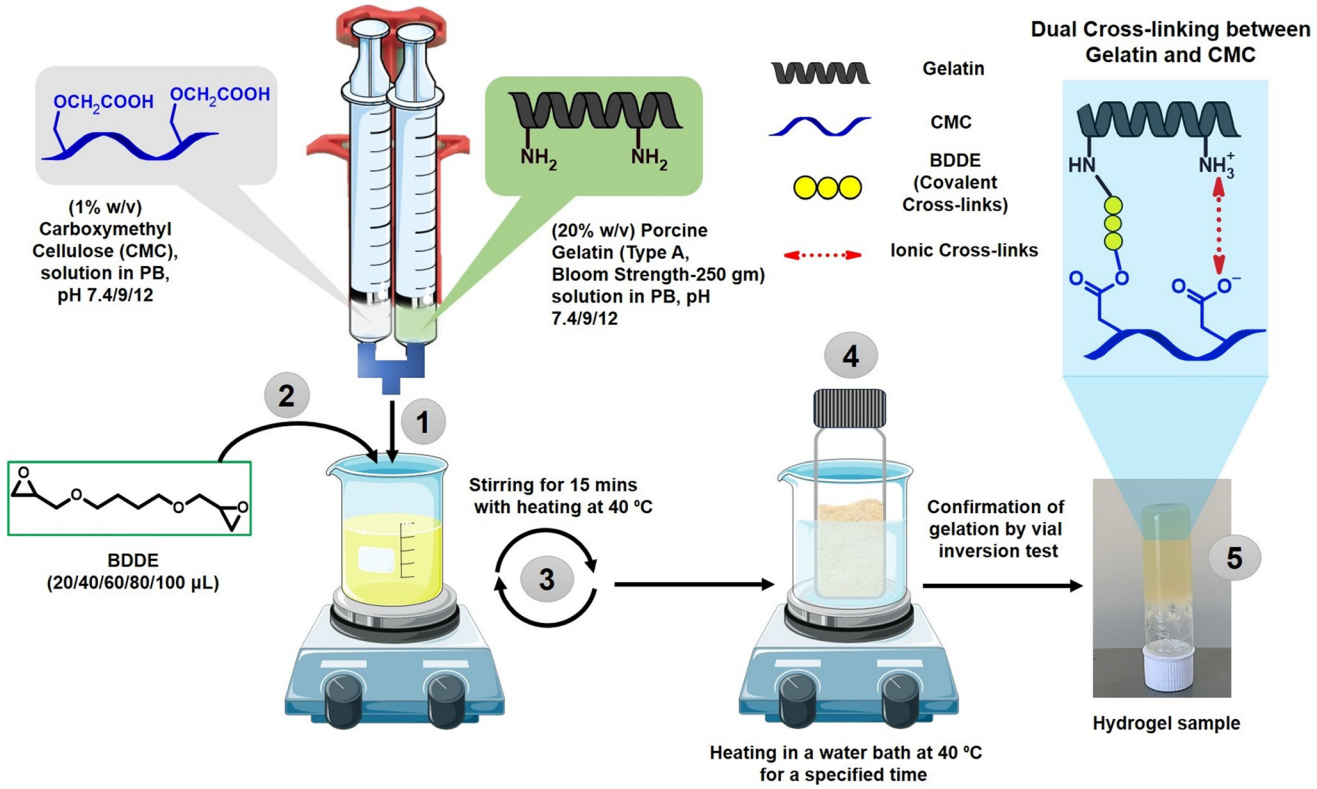

Fig. 2 General procedure to formulate pH-responsive hydrogels.

Table 1 Optimisation of gelation time as a function of volume ratio of CMC, gelatin and BDDE and pH

Types of gel	Volume of gelatin (mL) (20% w/v)	Volume of CMC (mL) (1% w/v)	Volume of BDDE (µL)	Volume ratio (CMC : gelatin : BDDE)	Gelation time* at pH 7.4, mean ± SD (h) (n = 3)	Gelation time* at pH 9, mean ± SD (h) (n = 3)	Gelation time* at pH 12, mean ± SD (h) (n = 3)
Gel-I	2	2	20	100 : 100 : 1	5.246 ± 0.18	3.176 ± 0.10	3.693 ± 0.28
Gel-II	2	2	40	50 : 50 : 1	5.02 ± 0.52	2.196 ± 0.14	3.873 ± 0.37
Gel-III	2	2	60	33.33 : 33.33 : 1	2.683 ± 0.31	2.183 ± 0.02	3.133 ± 0.12
Gel-IV	2	2	80	25 : 25 : 1	4.31 ± 0.12	2.223 ± 0.06	2.893 ± 0.35
Gel-V	2	2	100	20 : 20 : 1	4.323 ± 0.02	2.306 ± 0.06	2.643 ± 0.37

*Gelation time was calculated by the vial inversion method as per the previous reported methods.[82–84]

of phosphate buffer of three pH values (pH 4, pH 7.4 and pH 12) and incubated at 37 ± 1 °C for a period of 1 h. After 1 h, the gels were brought out, and then the diameter and height of the gels were measured for individual hydrogels. The volume of hydrogels (before swelling and after swelling/shrinking) was calculated by using the formula $\pi r^2 h$, where r and h are the radii and heights of cylindrical gels, respectively. The experiments were triplicated (n = 3), and the results are presented with mean values and standard deviations. The percentage of swelling/shrinking of the hydrogels is calculated using the following formula:

$$\%\,\text{swelling/shrinking} = \frac{\text{FV} - \text{IV}}{\text{IV}} \times 100 \qquad (1)$$

Here, FV = final volume of hydrogels and IV = initial volume of hydrogels.

Positive values show swelling, and negative values indicate shrinking of hydrogels.

2.5. Studies on the pH-responsiveness of hydrogels

Gel-III hydrogels were prepared and subjected to sequential immersion of the same hydrogel in buffer solutions of pH 12, pH 7.4 and pH 4 at 37 ± 1 °C for 1 h (in each buffer solution) to evaluate their pH-responsive swelling and shrinking behaviour. This sequential immersion cycle was repeated with a single gel three times from pH 12 to pH 4 and *vice versa*, keeping the mid-point at pH 7.4. The volume of the hydrogel is calculated after each immersion. The experiments were per-

formed in triplicate (n = 3), and the results are presented as mean values with standard deviations.

2.6. Biodegradability studies of hydrogels

The degradation profile of the prepared hydrogels was studied as per the ASTM standard, ASTM F1635-16 "Standard Test Method for *In Vitro* Degradation Testing of Hydrolytically Degradable Polymer Resins and Fabricated Forms for Surgical Implants". The biodegradability of hydrogels was studied by following the methods in the ASTM standard.[86]

2.6.1. Percentage weight reduction. Gel-III hydrogel samples were prepared using the method described in section 2.2. These hydrogel samples were dried at 50 °C for 24 h to get constant weights. These dried and weighed hydrogels were immersed in phosphate buffered saline (10 mL) and incubated with PBS at 37 ± 1 °C. After 1, 3, 5, 7, 15 and 21 days, the gels were removed from the PBS and dried for 24 h at 50 °C to get a constant weight. The % weight reduction was calculated using the following formula:

$$\text{Percentage weight loss} = \frac{\text{initial weight} - \text{weight after degradation}}{\text{initial weight}} \times 100 \quad (2)$$

2.6.2. Scanning electron microscopy (SEM). Scanning electron microscopy images of dried Gel-III samples were recorded to study the microscopic changes in hydrogels due to degradation. SEM images of Gel-III were recorded before degradation and after 21 days of degradation. Dried samples of Gel-III were examined by SEM (JEOL JSM-7610F Plus) after gold-coating for 60 s, and images were captured at a 2.00 kV acceleration voltage.

2.7. Rheology of hydrogels

To study the flow properties of the prepared hydrogels (Gel-III), rheology experiments were performed at 25 °C with a controlled stress rheometer (RheoCampass MCR302, Anton Paar) in cone plate geometry (25 mm diameter) with a 0.5 mm gap. An amplitude sweep experiment was performed from 0.1 to 1000% shear strain, and both of the moduli were recorded. Angular frequency sweep measurements were performed from 1 to 100 rad s^{-1} (at 1% shear strain), and both of the moduli were recorded.

2.8. Drug entrapment and pH-responsive drug release

Neomycin sulphate (NEO) was chosen as a model drug to study pH-responsive drug release at pH 6 and pH 9. These pH values were chosen for this study because of their direct correlation with disease conditions, such as pH 6 in the proximity of cancerous cells[20] while chronic wounds exhibit a pH of 9.[78] In this regard, using NEO for this study is relevant as it is a well-known antibiotic[87,88] and has also been reported to show anti-cancer activity.[89–91]

2.8.1. Drug entrapment in the hydrogel. 20% w/v and 1% w/v solutions of gelatin (Type A, bloom strength – 250 g) and CMC, respectively, were prepared in phosphate buffer (PB), pH 9. 2 mL of the gelatin solution was transferred to a vial, and 100 mg of neomycin sulphate (NEO) was dissolved in it under stirring at 40 °C. The gelatin solution containing NEO and CMC was loaded into a double-barrel syringe. The contents were co-injected into a clean beaker. Then, 60 μL of BDDE was added as a crosslinking agent to the polymeric solution, ensuring proper mixing of both solutions for 15 minutes under stirring at 40 °C. After mixing, the content was transferred into a vial, which was then placed in a water bath and heated to 40 °C to form the hydrogel with entrapped NEO.

2.8.2. Entrapment efficiency. Before proceeding to determine the entrapment efficacy of the hydrogel (Gel-III), it is a prerequisite to adopt a quantitative analytical method that helps determine the drug's concentration in a solution. We opted for UV-visible spectroscopy for this. Firstly, the solution of NEO was prepared in distilled water (5 mg mL^{-1}), and the absorption maximum was recorded at 305 nm. A series of standard solutions (1 mg mL^{-1}, 3 mg mL^{-1}, 5 mg mL^{-1}, 7 mg mL^{-1}, 9 mg mL^{-1}, and 11 mg mL^{-1}) was prepared, and the absorbance of each of the solutions was recorded at 305 nm. A standard curve was plotted between the concentration of NEO and absorbances of standard solutions of NEO to generate a straight-line equation as $Y = 0.0469X - 0.0155$, where $Y = \text{Abs}_{305\ \text{nm}}$ and X is the concentration of NEO (mg mL^{-1}) (Fig. S1).

Secondly, the Gel-III hydrogel loaded with NEO was placed in a beaker containing 10 mL of distilled water for 2 min to remove any surface-adsorbed NEO from the surface of the hydrogel. A sufficient aliquot was withdrawn to record the absorbance at 305 nm, and after processing using the straight-line equation, entrapment efficacy was calculated using the following formula:

$$\text{Entrapment efficacy}\ (\%) = \frac{\text{amount of NEO loaded in the hydrogel} - \text{adsorbed NEO on the hydrogel}}{\text{amount of NEO loaded in the hydrogel}} \times 100 \quad (3)$$

2.8.3. pH-Responsive drug release. After removing the surface-adsorbed NEO from Gel-III, Gel-III was transferred to a beaker containing 10 mL of PB solution at pH 9 and allowed to soak in the PB for 1 h at 37 ± 1 °C to study the drug (NEO) release. The absorbance of the PB (containing released NEO) was measured at 305 nm. Then, the NEO-loaded Gel-III was transferred into 10 mL of PB at pH 7.4 and allowed to soak in the PB for 1 h at 37 ± 1 °C. After 1 h, the hydrogel was removed, and an aliquot was collected to record the absorbance at 305 nm. After this, the gel was transferred into 10 mL of PB at pH 6 and allowed to soak in the PB (pH 6) for 1 h at 37 ± 1 °C. The NEO-loaded gel was removed, and an aliquot was collected to record the absorbance at 305 nm. Likewise, the same gel was exposed to different pH environments (buffer solutions) (*e.g.* pH 7.4 → pH 9 → pH 7.4 → pH 6) for 1 h at 37 ± 1 °C, and after each step, the absorbances of the buffer solutions were recorded at 305 nm. Thus, the obtained absorption

values (which directly correlated with NEO conc.) were plotted against the pH values. Additionally, the volume of the NEO-loaded Gel-III was also calculated at each step and was plotted against pH values as per the procedure mentioned in section 2.5.

2.9. Cytocompatibility study (MTT assay)

A study of the cytocompatibility of the prepared hydrogel was performed using the MTT assay as per the previously reported method with some modifications.[51] In brief, the hydrogel samples, Gel-III (25 μg and 50 μg), were incubated for 0, 1, 3, 5 and 7 days in 1 mL of Dulbecco's modified Eagle's medium (DMEM), supplemented with 10% (w/v) fetal bovine (calf) serum, 100 IU mL^{-1} penicillin, and 100 μg mL^{-1} streptomycin at 37 °C to extract the degraded and leached products. HeLa cells were seeded into 96-well plates, maintained and cultured in DMEM supplemented with 10% (w/v) fetal bovine serum, 100 IU mL^{-1} penicillin, and 100 μg mL^{-1} streptomycin at 37 °C under a humidified atmosphere with 5% CO_2 in a CO_2 incubator for 24 h (~1 doubling period) to form a semi-confluent monolayer: 1×10^4 cells per 100 μL of MEM/well. The culture medium was removed by aspiration. 100 μL of the hydrogel extract (withdrawn at each time point) was added to the medium and incubated at 37 °C, 5% CO_2 for 24 h. The cells were evaluated microscopically to observe any morphological alterations. The culture medium was removed by aspiration. 50 μL of sterilised MTT (5 mg mL^{-1}) stock solution in phosphate buffered saline (PBS) was added to each well and incubated for 3 h. After 2 h, the MTT solution was decanted, and formazan crystals that could be seen under the microscope were dissolved in 50 μL of DMSO. This plate was shaken slowly, and subsequently transferred to a microplate reader, and the absorbance was measured at 570 nm. Absorbance is directly correlated with a higher number of viable cells. Percentage cell viability can be determined using the following formula:

$$\text{Percentage cell viability} = \frac{\text{OD (570) test}}{\text{OD (570) blank}} \times 100 \quad (4)$$

OD (570) test is the mean value of the measured optical density of the extracts of the hydrogel samples. OD (570) blank is the mean value of the measured optical density of the blank.

3. Results and discussion

3.1. Formulation and optimisation of hydrogels: insight into internal cross-linking

Different volume ratios of gelatin solution (20% w/v), CMC solution (1% w/v) and BDDE were employed at different pH values of 7.4, 9 and 12 to get the lowest gelation time (the results are summarised in Table 1). Among all three pH values, gelation at pH 9 showed the relatively shortest gelation time at each of the BDDE concentrations. This happens because at this pH, electrostatic interactions remain optimum and suitable for dual cross-linking (Fig. 1). Electrostatic interaction is the primary force to bring gelatin (positively charged polyelectrolyte) and CMC (negatively charged polyelectrolyte) into proximity. This proximity of both of the counter polyelectrolytes at this pH promotes covalent cross-linking between these oppositely charged PEs with added BDDE molecules. At pH 9, the close vicinity of the primary amines of lysine groups of gelatin and carboxylate ions of CMC tends to react with the epoxide rings of BDDE.[92,93] This was confirmed by the FTIR spectrum of the dried powder of the hydrogel (GEL-III). In this spectrum (Fig. S5; SI), a peak around 1779 cm^{-1} suggests carbonyl groups in the ester groups formed by the cross-linking of –COONa of CMC with BDDE.[85] Peaks for secondary amines around 3300 cm^{-1} resulted from the reaction of the primary amine of gelatin and the epoxy rings of BDDE and might have merged with peaks of the other compounds (*e.g.* CMC) present in the xerogel (Fig. S5; SI).[59] Hence, gelatin (cationic PE) and CMC (anionic PE) get cross-linked to generate a 3D hydrogel network.

At pH 7.4, gelation takes more time as compared to the gelation at pH 9 and at pH 12. However, at this pH, gelatin and CMC tend to behave as cationic and anionic PEs, respectively, and provide the primary force of interaction through electrostatic interaction too. Nevertheless, neutral/mild basic pH does not greatly favour the reaction between the primary amine (of gelatin) and BDDE to cross-link with CMC.[93] This holds true as a larger population of primary amines of gelatin remains protonated at this pH[15] and has less tendency to react with BDDE.[93]

However, we observed that the addition of 60 μL of BDDE suddenly decreased the gelation time (Fig. 3), which may be due to a higher availability of BDDE or because a higher amount of BDDE may cross-link CMC chains only.[94] Interestingly, further increasing the BDDE amount to 80 μL and 100 μL may lead to an overly dense network. Excessive crosslinking can limit the mobility of polymer chains, restricting their ability to rearrange and form a gel. This can result in increased gelation time with 80 and 100 μL of BDDE.[60,95]

At pH 12, gelatin type A bears a negative charge (the isoelectric point of gelatin type A is 7–9); thus, it behaves as an

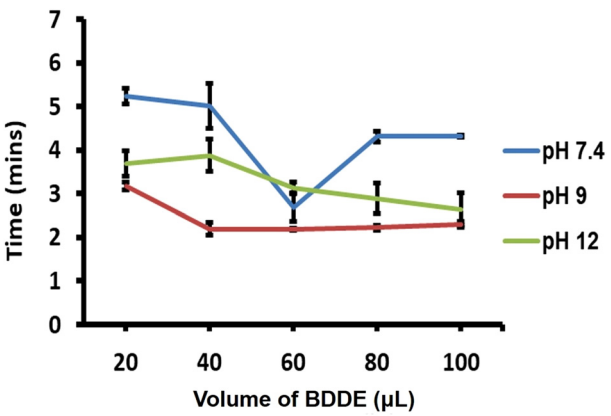

Fig. 3 Gelation time of hydrogels as a function of pH and volume of BDDE.

anionic polyelectrolyte.[96,97] Hence, at pH 12, gelatin and CMC both behave as anionic polyelectrolytes and do not have electrostatic attraction. Lacking the primary gelation force, both components (gelatin and CMC) can still undergo covalent cross-linking through BDDE with a reduced rate of reaction, which leads to a higher gelation time than that at pH 9 (Fig. 3).

3.2. Swelling/shrinking behaviour of hydrogels

The pH-Responsive swelling and shrinking behaviour of hydrogels is a critical property that makes them a potential platform for pH-responsive drug delivery. This behaviour is governed by the interaction between the polymeric functional groups and the surrounding pH.[10,98] The proposed hydrogel exhibited bi-directional pH-responsive swelling. Gel-III showed around 58% and 61% swelling at pH 4 and pH 12, respectively, at 37 °C within 1 h. Contrary to this, Gel-III showed around 61% shrinking at pH 7.4 at 37 °C within 1 h (Fig. 4). Thus, the prepared hydrogel responds to pH values below and above the physiological pH 7.4 and is hence called a bi-directional pH-responsive hydrogel. This bi-directional pH-dependent swelling and shrinking behaviour of the prepared hydrogels is attributed to the dual cross-linking of gelatin and CMC: the first one is pH-dependent ionic cross-linking and the second one is stable BDDE-based covalent cross-linking (Fig. 2 and 4b). At pH 4, carboxylic groups of CMC remain protonated (–COOH);[22] thus, CMC does not carry a negative charge to interact with positively charged gelatin. At this pH, gelatin and CMC are connected through BDDE cross-links only. In this case, when Gel-III is immersed in the pH 4 medium, water molecules enter the hydrogel and exert osmotic pressure. This results in significant swelling of the gel, especially in the absence of electrostatic interaction between gelatin and CMC (Fig. 4a). At pH 12, amine groups of gelatin remain deproto-

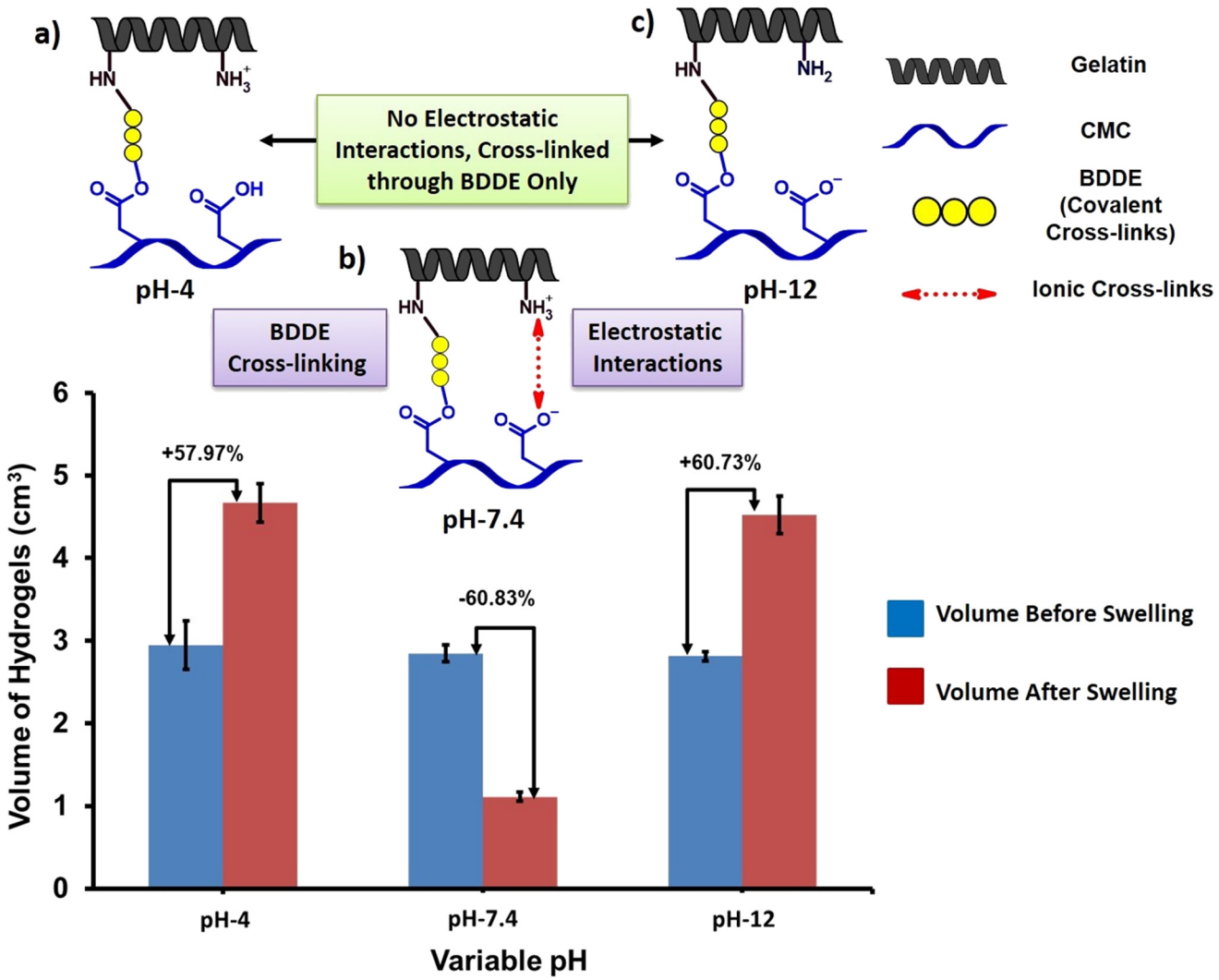

Fig. 4 Bar graph of swelling/shrinking behaviour of the hydrogel (Gel-III) as a function of pH along with associated cross-linking: (a) at pH 4 and (c) at pH 12, gel and CMC are cross-linked through BDDE only, not by ionic interactions; (b) at pH 7.4, gel and CMC are cross-linked through BDDE and ionic interactions.

nated (uncharged) ($-NH_2$);[15] thus, gelatin does not carry a positive charge to interact with negatively charged CMC. At this pH, gelatin and CMC are connected through BDDE cross-links only. In this case, when Gel-III is immersed in the pH 12 medium, water molecules enter the hydrogel and exert osmotic pressure. This results in significant swelling of the gel, especially in the absence of electrostatic interactions between gelatin and CMC (Fig. 4c).

In contrast to both of the above-mentioned cases, when Gel-III is immersed in the pH 7.4 medium and allowed to reach equilibrium at pH 7.4, the amine groups of gelatin become protonated (charged) ($-NH^{3+}$) and the carboxylic groups of CMC become deprotonated ($-COO^-$).[15,22] Thus, at this pH, gelatin, which carries a positive charge, starts interacting with negatively charged CMC through ionic interactions. Restoration of electrostatic interactions between gelatin and CMC, which are already connected through BDDE cross-links, results in the shrinking of Gel-III. In this case, the exerted osmotic pressure is superseded by dual cross-linking; hence, we see about 61% shrinking in Gel-III rather than swelling (Fig. 4b).

3.3. pH-Responsiveness of hydrogels

After studying the pH-dependent swelling/shrinking behaviour, we investigated the effect of three reversible cycles of pH change to evaluate the reversible pH responsiveness (swelling/shrinking behaviour) of a single sample of hydrogel, Gel-III. Gel-III exhibited prominent swelling after experiencing pH 12 (points B and F, Fig. 5) and pH 4 (points D and H, Fig. 5) environments. As discussed earlier, this happens due to compromised electrostatic bonding between gelatin and CMC at pH 12 and pH 4. Transferring the same hydrogel sample to PB pH 7.4 intermittently resulted in significant shrinking (points C, E and G, Fig. 5). Thus, the produced shrinkage was attributable to the restoration of electrostatic (ionic) attraction between the ammonium ions of gelatin and the carboxylate ions of CMC at pH 7.4. This experiment confirms the repetitive bi-directional pH-sensitive swelling, which strongly advocates that this same hydrogel platform may be utilised for delivering the drugs in acidic and basic environments.

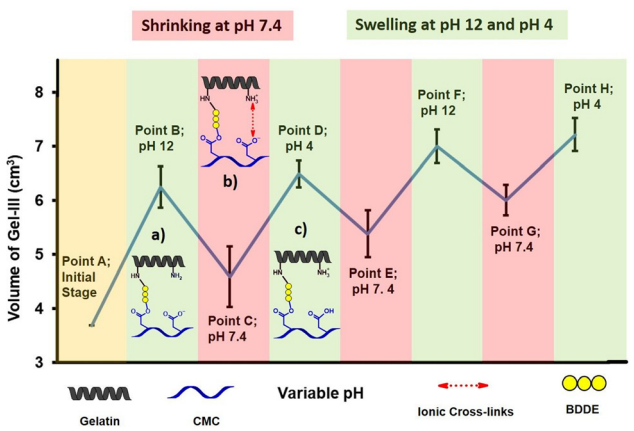

Fig. 5 pH-Induced swelling–shrinking cycle of a single Gel-III hydrogel sample. Embedded figures (a), (b) and (c) represent types of cross-linking between gelatin and CMC, at pH 12, 7.4 and 4.

3.4. Rheology of hydrogels

The rheological profile of the prepared hydrogel can be employed to evaluate the flow properties. Judicious fluidity/modulus controls the ease of handling/applicability of the hydrogel on the biological surfaces. Firstly, the fluidity of hydrogel Gel-III was evaluated by calculating the storage modulus (G') and loss modulus (G'') of the hydrogel by conducting an amplitude sweep experiment. The amplitude (strain) sweep experiment showed that the prepared hydrogel (Gel-III) can tolerate 0.1–100% strain (upper panel; Fig. 6). This suggests that the prepared hydrogel is robust enough to handle during transportation and transfer from packaging to the application site.[99]

The storage modulus of the gel remains higher than the loss modulus before the gel breaking point at 1000% strain. Secondly, the frequency sweep experiment showed that the G' value was higher than the G'' value over the frequency range of 1–100 rad s^{-1} (lower panel; Fig. 6). These results confirm the gel-like character of the prepared hydrogel over the frequency range (1–100 rad s^{-1}) and indicate that it maintains its internal structure under substantial applied strain.

3.5. Biodegradability studies

The biodegradability of the prepared hydrogel is a crucial attribute for biomedical applications. We found that Gel-III underwent 90% weight reduction in 21 days in phosphate buffer at pH 7.4 and 37 °C (Fig. 7). This degradation profile looks promising for wound healing applications due to similar time points being involved for wound/skin repair and the hydrogel's degradation.[100] The degradation of the hydrogel (Gel-III) was further assured at the microscopic level, also by SEM studies before and after degradation (Fig. 7; inset images). The captured SEM micrographs confirm the surface erosion through the formation of fluffy and expanded bulges during the degradation of the hydrogels.

3.6. Scanning electron microscopy (SEM) of the prepared hydrogels

SEM micrographs of the Gel-III hydrogel were recorded before degradation and after 21 days (after ~90% degradation) to study the effect of degradation on the morphology of hydrogel samples. The SEM micrograph of an intact (before degradation) hydrogel sample shows a comparatively smooth (no fluffy bulges) surface, even at 5000× magnification (Fig. 8a; inset image), while the degraded hydrogel sample shows fluffy bulges pointing outwards (Fig. 8b; yellow arrows and lines), which may be due to the hydrogel surface being stretched by osmotic pressure during degradation. These results are consistent with earlier published reports regarding hydrogel swelling and degradation.[100–102]

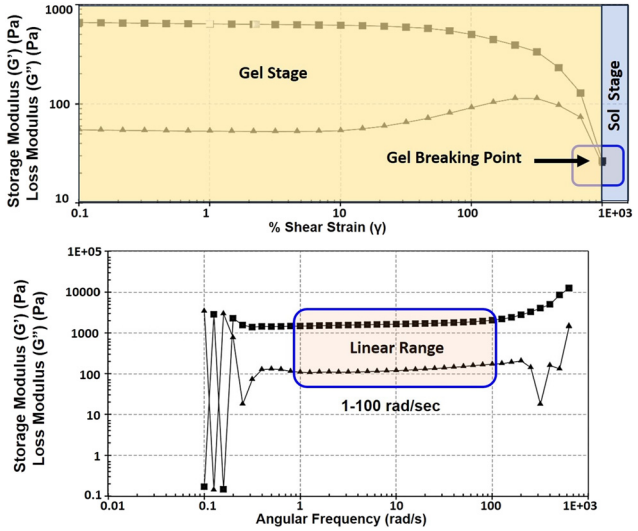

Fig. 6 Upper panel: amplitude (strain) sweep (from 0.1 to 1000%) rheological study of hydrogel Gel-III. Lower panel: frequency sweep (from 0.1 to 1000 rad s^{-1} frequency) rheological study of hydrogel Gel-III at 1% strain.

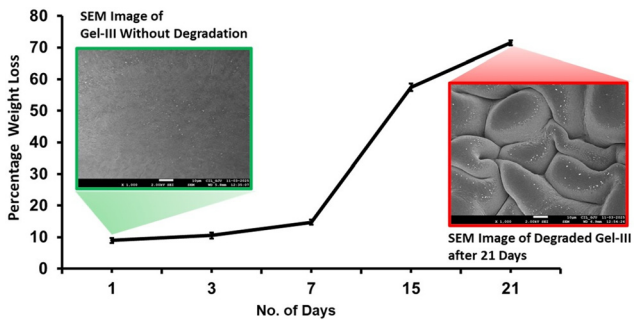

Fig. 7 Degradation profile of the hydrogel (Gel-III) obtained by the percentage weight reduction method according to the ASTM F1635-16 protocol and by observing the corresponding SEM macroscopic images (inset images). Surface bulging was observed in SEM micrographs of the degraded hydrogel (Gel-III).

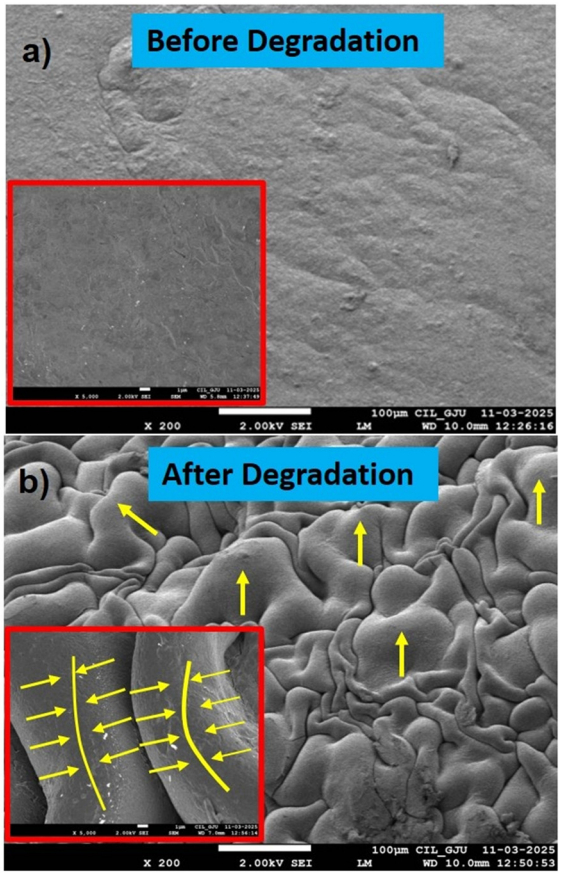

Fig. 8 Representative SEM micrographs of (a) the hydrogel sample Gel-III before degradation, showing a flat surface; and (b) after 21 days of degradation, showing multiple bulges on the surface of the hydrogel. Images in insets (in red rectangles) are magnified images of the respective micrographs. The yellow arrows and lines show prominent bulges due to degradation.

3.7. Drug entrapment and release

We then probed the applicability of this hydrogel towards a bi-directional pH-responsive drug delivery application. For this exploration, we selected two pH values, 6 and 9 (below and above physiological pH, respectively) for pH-responsive drug release because the vicinity of tumour cells has a pH around 6, while basic pH 9 prevails in the proximity of chronic wounds.[20,78] The prepared gel, Gel-III, could efficiently incorporate the antibiotic drug neomycin sulphate (NEO), which additionally has shown some anti-cancer effects.[89–91] NEO could be entrapped with 84% efficiency. This excellent entrapment efficiency is attributed to ionic interactions between the ammonium groups (NH_3^+) of NEO and the carboxylate groups (COO^-) of CMC at physiological pH (7.4). These ionic interactions prevail around pH 7.4 but become weaker at pH 9 and 6. This happens because, as compared to pH 7.4, a lower proportion of primary amines remains protonated (positively charged) at pH 9, while a lower proportion of carboxylate anion is available at pH 6. These reduced ionic interactions between NEO and CMC at pH 6 and 9 contribute to the release of NEO from the hydrogel.

This hypothesis is nicely reflected in the changes in absorbance values (at 305 nm) of released NEO at pH 6 and pH 9 as compared to the absorbance values at pH 7.4 (Fig. 9a). This trend strongly suggests that entrapped NEO can be released in greater quantities in PB of pH 6 and pH 9 as compared to pH 7.4. This release profile follows the swelling and shrinking behaviour of the hydrogel, where pH 6 and pH 9 exhibit swelling and pH 7.4 results in the shrinking of the hydrogel (Fig. 9b). Following the discussion in section 3.3, at pH 7.4, electrostatic interactions between gelatin and CMC remain more prominent than at pH 6 and pH 9 (BDDE cross-links remain constant for all three pH values). At pH 6 and pH 9, lower levels of ionic interactions between gelatin and CMC allow the hydrogel to swell due to osmotic pressure. This swell-

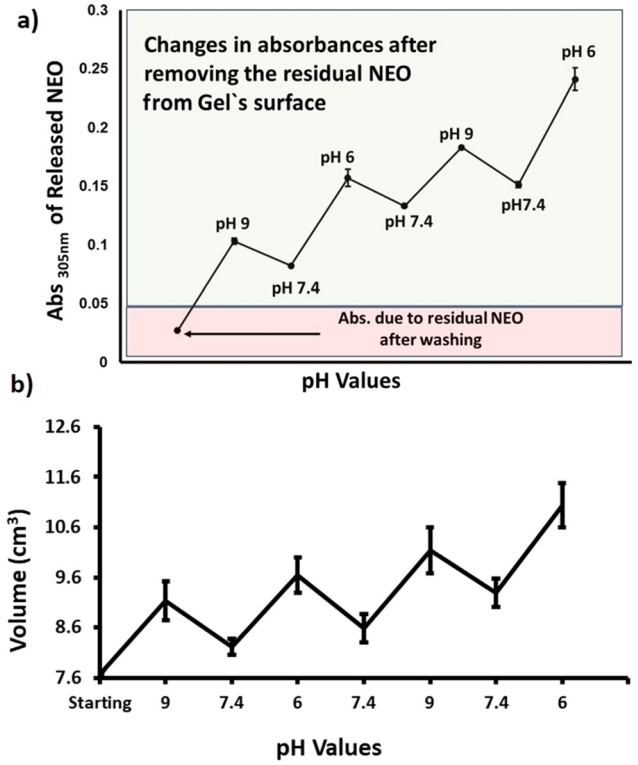

Fig. 9 (a) Repeated pH-responsive release of neomycin sulphate (NEO); (b) analogous pH-responsive swelling and shrinking behaviour of the hydrogel sample Gel-III.

ing, along with the subdued ionic interactions with NEO and CMC, result in a greater release of NEO at both pH values. On the other hand, at pH 7.4, a higher level of electrostatic interactions between gelatin and CMC forces the hydrogel to shrink. In addition to the shrinkage of the hydrogel at pH 7.4, strong ionic interactions between NEO and CMC at this pH value restrict the drug release, which is reflected by lower absorbance values at 305 nm. A few controversial and divergent hypotheses about drug release, such as degradation-induced release and diffusion-induced release, can be ruled out in this case.[103] In the first case, the entrapped drug NEO is released as a function of pH only within a 24 h period where degradation of the hydrogel is negligible, while in the second case, NEO can be released after charge neutralisation (of either CMC or NEO) and osmotic pressure, rather than by diffusion only. Thus, observations of these experiments strongly suggest the potential of the prepared hydrogels for bi-directional, on-demand pH-responsive drug delivery at both clinically relevant pH values.

3.8. Cytocompatibility studies

The prepared hydrogel sample (Gel-III) was found to show around 100% cell viability for HeLa cell lines up to 7 days at 25 μg mL^{-1} and 50 μg mL^{-1} (Fig. 10). These results reconfirm the biocompatibility of gelatin, CMC and BDDE.[59,104,105]

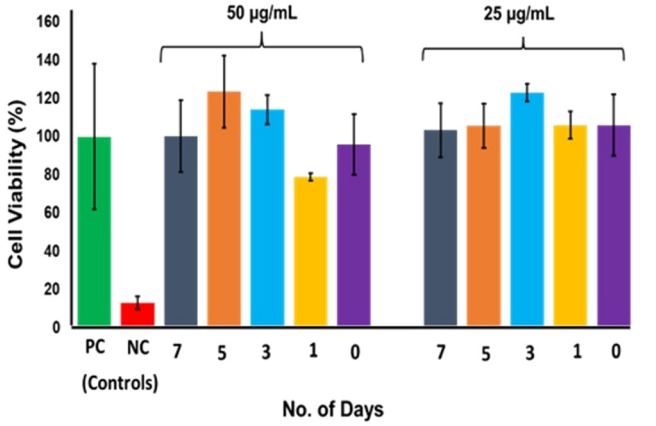

Fig. 10 Percentage cell viability of the hydrogel sample Gel-III after different numbers of days of incubation with HeLa cells. HeLa cells, along with media without any hydrogel sample, were taken as a positive control and Triton X-100 was taken as a negative control.

4. Conclusion

In conclusion, we have demonstrated the development of a bi-directional pH-responsive hydrogel platform for drug delivery. These hydrogels are fabricated from oppositely charged polyelectrolytes and have dual cross-linking; one is pH-dependent ionic cross-linking, while the other is BDDE-based covalent cross-linking. These hydrogels reversibly respond to both acidic and basic pH values and deliver the entrapped drug effectively. The hydrogels are biodegradable, and all their components are FDA approved. Optimisation of the BDDE content in the hydrogel Gel-III afforded the shortest gelation time. The hydrogel degraded on its own in about three weeks. The drug-delivery potential of this hydrogel was shown by the pH-assisted release of entrapped neomycin sulphate in acidic and basic environments. The formulation of this pH-responsive hydrogel system does not require any special equipment and is free from organic solvents. All the components (gelatin, CMC and BDDE) of the proposed hydrogel system are cost-effective, although this hydrogel system may face some limitations, such as being usable efficiently for a shorter period of time only, due to its 90% degradation occurring within 21 days. Another minor challenge it may face is the requirement for the fabrication of a larger double-barrel container with suitable mixers to mix CMC and gelatin. Considering all the pros and cons, we believe that the proposed hydrogel is suitable for scaling up.

Conflicts of interest

The authors declare that they have no conflicts of interest.

Data availability

The data supporting this article have been included as part of the supplementary information (SI). Supplementary infor-

mation: standard curve of neomycin sulphate (NEO) in water; Tables S1–S3; FTIR spectra of gelatin, CMC, BDDE and dried hydrogel formulation Gel-III. See DOI: https://doi.org/10.1039/d6pm00077k.

Acknowledgements

The authors are thankful to GD Goenka University, Sohna, for infrastructure support. They are also thankful to Dr Rajendra Kurapati, Indian Institute of Science Education and Research, Thiruvananthapuram, for conducting cell cytotoxicity studies in his laboratory.

References

1 J. Li and D. J. Mooney, *Nat. Rev. Mater.*, 2016, **1**, 1–17.
2 R. Narayanaswamy and V. P. Torchilin, *Molecules*, 2019, **24**, 603.
3 S. J. Buwalda, T. Vermonden and W. E. Hennink, *Biomacromolecules*, 2017, **18**, 316–330.
4 M. Rizwan, R. Yahya, A. Hassan, M. Yar, A. Azzahari, V. Selvanathan, F. Sonsudin and C. Abouloula, *Polymers*, 2017, **9**, 137.
5 A. Bordbar-Khiabani and M. Gasik, *Int. J. Mol. Sci.*, 2022, **23**, 3665.
6 Y. Li, X. Ding, H. Hu and F.-J. Xu, *Precis. Med. Eng.*, 2024, **1**, 100001.
7 A. Alsuraifi, A. Curtis, D. A. Lamprou and C. Hoskins, *Pharmaceutics*, 2018, **10**, 136.
8 L. P. Tricou, M. L. Al-Hawat, K. Cherifi, G. Manrique, B. R. Freedman and S. Matoori, *Adv. Wound Care*, 2024, **13**, 446–462.
9 Y. Liu, W. Kang, L. Nie, F. Xiao, Y. Li, Q. Ma, D. Lin, G. Zhou, S. Liu, K. Sun and X. Li, *React. Funct. Polym.*, 2024, **204**, 106025.
10 P. Gupta, K. Vermani and S. Garg, *Eur. J. Pharm. Sci.*, 2002, **15**, 187–192.
11 G. Kocak, C. Tuncer and V. Bütün, *Polym. Chem.*, 2017, **8**, 144–176.
12 K. Lavanya, S. V. Chandran, K. Balagangadharan and N. Selvamurugan, *Mater. Sci. Eng., C*, 2020, **106**, 110862.
13 Y. Che, D. Li, Y. Liu, Q. Ma, Y. Tan, Q. Yue and F. Meng, *RSC Adv.*, 2016, **6**, 106648–106655.
14 M. Mahdian, S. Akbari Asrari, M. Ahmadi, T. Madrakian, N. Rezvani Jalal, A. Afkhami, M. Moradi and L. Gholami, *J. Drug Delivery Sci. Technol.*, 2023, **84**, 104537.
15 Z. Cimen, S. Babadag, S. Odabas, S. Altuntas, G. Demirel and G. B. Demirel, *ACS Appl. Polym. Mater.*, 2021, **3**, 3504–3518.
16 S. Bahmani, R. Khajavi, M. Ehsani, M. K. Rahimi and M. R. Kalaee, *Int. J. Biol. Macromol.*, 2025, **284**, 138034.
17 X. Shi, M. Lan, J. Liu, J. Zhou and H. Gu, *Polymer*, 2024, **308**, 127365.
18 S. Setoyama, R. Haraguchi, S. Aoki, Y. Oishi and T. Narita, *Int. J. Mol. Sci.*, 2024, **25**, 10439.
19 J. Yang, Z. Zhu, J. Zhang, C. Chen, Z. Lei, L. Li, Z. Feng and X. Su, *J. Polym. Res.*, 2023, **30**, 1–9.
20 Y. Wu, Y. Li, R. Han, Z. Long, P. Si and D. Zhang, *Biomacromolecules*, 2023, **24**, 5364–5370.
21 T. Thambi, J. M. Jung and D. S. Lee, *Biomater. Sci.*, 2023, **11**, 1948–1961.
22 R. R. Mohamed, M. E. Fahim and S. M. A. Soliman, *BMC Chem.*, 2022, **16**, 1–12.
23 D. S. Lima, E. T. Tenório-Neto, M. K. Lima-Tenório, M. R. Guilherme, D. B. Scariot, C. V. Nakamura, E. C. Muniz and A. F. Rubira, *J. Mol. Liq.*, 2018, **262**, 29–36.
24 T. S. Anirudhan, M. Mohan and M. R. Rajeev, *Int. J. Biol. Macromol.*, 2022, **201**, 378–388.
25 H. Suo, M. Hussain, H. Wang, N. Zhou, J. Tao, H. Jiang and J. Zhu, *Biomacromolecules*, 2021, **22**, 3049–3059.
26 A. R. Simão, V. H. Fragal, A. M. de O. Lima, M. C. G. Pellá, F. P. Garcia, C. V. Nakamura, E. B. Tambourgi and A. F. Rubira, *Int. J. Biol. Macromol.*, 2020, **148**, 302–315.
27 C. Chang, M. He, J. Zhou and L. Zhang, *Macromolecules*, 2011, **44**, 1642–1648.
28 S. H. Park, H. S. Shin and S. N. Park, *Carbohydr. Polym.*, 2018, **200**, 341–352.
29 J. S. Vuković, M. Žabčić, L. Gazvoda, M. Vukomanović, T. R. Ilić-Tomić, D. R. Milivojević and S. L. Tomić, *Biopolymers*, 2025, **116**, e70008.
30 P. S. Yavvari, A. K. Awasthi, A. Sharma, A. Bajaj and A. Srivastava, *J. Mater. Chem. B*, 2019, **7**, 2102–2122.
31 B. Gyarmati, Á. Némethy and A. Szilágyi, *RSC Adv.*, 2014, **4**, 8764–8771.
32 S. Nesrinne and A. Djamel, *Arabian J. Chem.*, 2017, **10**, 539–547.
33 X. Gao, C. He, C. Xiao, X. Zhuang and X. Chen, *Polymer*, 2013, **54**, 1786–1793.
34 R. Pappalardo, M. Boffito, C. Cassino, V. Caccamo, V. Chiono and G. Ciardelli, *ACS Omega*, 2024, **9**, 25609–25621.
35 F. Hakimi, L. Maeso, A. Dehghan, A. Dolatshahi-Pirouz, G. M. Stojanovic, M. Stojanovic, M. Nadimifar, Z. Ahmadian and G. Orive, *ChemistrySelect*, 2025, **10**, e05175.
36 S. Li, M. Pei, T. Wan, H. Yang, S. Gu, Y. Tao, X. Liu, Y. Zhou, W. Xu and P. Xiao, *Carbohydr. Polym.*, 2020, **250**, 116922.
37 H. Su, R. Zheng, L. Jiang, N. Zeng, K. Yu, Y. Zhi and S. Shan, *Carbohydr. Polym.*, 2021, **265**, 118085.
38 V. T. Tran, M. T. I. Mredha, J. Y. Na, J. K. Seon, J. Cui and I. Jeon, *Chem. Eng. J.*, 2020, **394**, 124941.
39 K. Yang, K. Wei, M. de Lapeyrière, K. Maniura-Weber and M. Rottmar, *Cell Rep. Phys. Sci.*, 2024, **5**, 101809.
40 H. Ding, B. Li, Y. Jiang, G. Liu, S. Pu, Y. Feng, D. Jia and Y. Zhou, *Carbohydr. Polym.*, 2021, **251**, 117101.
41 S. Summonte, G. F. Racaniello, A. Lopedota, N. Denora and A. Bernkop-Schnürch, *J. Controlled Release*, 2021, **330**, 470–482.

42 L. J. Macdougall, M. M. Pérez-Madrigal, M. C. Arno and A. P. Dove, *Biomacromolecules*, 2018, **19**, 1378–1388.
43 S. Yigit, R. Sanyal and A. Sanyal, *Chem. – Asian J.*, 2011, **6**, 2648–2659.
44 T. M. FitzSimons, E. V. Anslyn and A. M. Rosales, *ACS Polym. Au*, 2021, **2**, 129–136.
45 A. Andersen, M. Krogsgaard and H. Birkedal, *Biomacromolecules*, 2018, **19**, 1402–1409.
46 F. Lee, K. H. Bae and M. Kurisawa, *Biomed. Mater.*, 2016, **11**, 014101.
47 H. Pan, Y. Qu, F. Wang, S. Zhao and G. Chen, *Colloid Interface Sci. Commun.*, 2025, **66**, 100828.
48 R. Wakabayashi, W. Ramadhan, K. Moriyama, M. Goto and N. Kamiya, *Polym. J.*, 2020, **52**, 899–911.
49 J. R. Clegg, K. Adebowale, Z. Zhao and S. Mitragotri, *Bioeng. Transl. Med.*, 2024, **9**, e10680.
50 M. Ahangarpour, I. Kavianinia and M. A. Brimble, *Org. Biomol. Chem.*, 2023, **21**, 3057–3072.
51 T. N. Pham, C. F. Su, C. C. Huang and J. S. Jan, *Colloids Surf., B*, 2020, **196**, 111316.
52 B. Liu, L. Burdine and T. Kodadek, *J. Am. Chem. Soc.*, 2006, **128**, 15228–15235.
53 M. Krogsgaard, M. A. Behrens, J. S. Pedersen and H. Birkedal, *Biomacromolecules*, 2013, **14**, 297–301.
54 J. W. Bae, J. H. Choi, Y. Lee and K. D. Park, *J. Tissue Eng. Regen. Med.*, 2015, **9**, 1225–1232.
55 G. Yang, Z. Xiao, X. Ren, H. Long, H. Qian, K. Ma and Y. Guo, *PeerJ*, 2016, **2016**, e2497.
56 A. Sharma, S. Kundu, A. Reddy M, A. Bajaj and A. Srivastava, *Macromol. Biosci.*, 2013, **13**, 927–937.
57 A. Sharma, T. Dutta and A. Srivastava, *Chem. – Eur. J.*, 2024, **30**, e202302157.
58 G. Mugnaini, R. Gelli, L. Mori and M. Bonini, *ACS Appl. Polym. Mater.*, 2023, **5**, 9192–9202.
59 K. De Boulle, R. Glogau, T. Kono, M. Nathan, A. Tezel, J. X. Roca-Martinez, S. Paliwal and D. Stroumpoulis, *Dermatol. Surg.*, 2013, **39**, 1758–1766.
60 J. A. Del Olmo, L. Pérez-álvarez, V. S. Martínez, S. B. Cid, R. P. González, J. L. Vilas-Vilela and J. M. Alonso, *Gels*, 2022, **8**, 223.
61 G. Martínez-Mejía, N. A. Vázquez-Torres, A. Castell-Rodríguez, J. M. del Río, M. Corea and R. Jiménez-Juárez, *Colloids Surf., A*, 2019, **579**, 123658.
62 I. H. Yang, I. E. Lin, T. C. Chen, Z. Y. Chen, C. Y. Kuan, J. N. Lin, Y. C. Chou and F. H. Lin, *Carbohydr. Polym.*, 2021, **260**, 117832.
63 B. B. Pinheiro, N. S. Rios, E. Rodríguez Aguado, R. Fernandez-Lafuente, T. M. Freire, P. B. A. Fechine, J. C. S. dos Santos and L. R. B. Gonçalves, *Int. J. Biol. Macromol.*, 2019, **130**, 798–809.
64 J. R. Dias, S. Baptista-Silva, C. M. T. de Oliveira, A. Sousa, A. L. Oliveira, P. J. Bártolo and P. L. Granja, *Eur. Polym. J.*, 2017, **95**, 161–173.
65 M. Chauhan, P. Roopmani, J. Rajendran, K. P. Narayan and J. Giri, *Int. J. Biol. Macromol.*, 2025, **285**, 138200.
66 X. Li, W. Xue, C. Zhu, D. Fan, Y. Liu and M. Xiaoxuan, *Mater. Sci. Eng., C*, 2015, **57**, 189–196.
67 X. Wu, L. Black, G. Santacana-Laffitte and C. W. Patrick, *J. Biomed. Mater. Res., Part A*, 2007, **81**, 59–65.
68 J. She, J. Liu, Y. Mu, S. Lv, J. Tong, L. Liu, T. He, J. Wang and D. Wei, *React. Funct. Polym.*, 2025, **207**, 106136.
69 S. Khunmanee, Y. Jeong and H. Park, *J. Tissue Eng.*, 2017, **8**, 2041731417726464.
70 G. Buhus, M. Popa and J. Desbrieres, *J. Bioact. Compat. Polym.*, 2009, **24**, 525–545.
71 D. Sala, F. Di Gennaro, M. Makvandi, P. Borzacchiello, W. Ji, F. Della Sala, M. Di Gennaro, P. Makvandi and A. Borzacchiello, *Gels*, 2024, **10**, 67.
72 A. Sannino, M. Madaghiele, F. Conversano, G. Mele, A. Maffezzoli, P. A. Netti, L. Ambrosio and L. Nicolais, *Biomacromolecules*, 2004, **5**, 92–96.
73 V. M. de Oliveira Cardoso, B. Stringhetti Ferreira Cury, R. C. Evangelista and M. P. Daflon Gremião, *J. Mech. Behav. Biomed. Mater.*, 2017, **65**, 317–333.
74 J. Faivre, A. I. Pigweh, J. Iehl, P. Maffert, P. Goekjian and F. Bourdon, *Expert Rev. Med. Devices*, 2021, **18**, 1175–1187.
75 Y. Privar, A. Skatova, M. Maiorova, A. Golikov, A. Boroda and S. Bratskaya, *Gels*, 2024, **10**, 483.
76 Z. Peng, Z. Peng and Y. Shen, *Polym.-Plast. Technol. Eng.*, 2011, **50**, 1160–1164.
77 G. Patroklou, E. Triantafyllopoulou, P. E. Goula, V. Karali, M. Chountoulesi, G. Valsami, S. Pispas and N. Pippa, *Polymers*, 2025, **17**, 1451.
78 L. P. Tricou, M. L. Al-Hawat, K. Cherifi, G. Manrique, B. R. Freedman and S. Matoori, *Adv. Wound Care*, 2024, **13**, 446–462.
79 F. Della Sala, M. di Gennaro, P. Makvandi and A. Borzacchiello, *Gels*, 2024, **10**, 67.
80 M. Wojtkiewicz, A. Stachura, B. Roszkowski, N. Winiarska, K. Kazimierska and K. Stachura, *Aesthetic Plast. Surg.*, 2024, **48**, 5147–5154.
81 A. Ahmady and N. H. Abu Samah, *Int. J. Pharm.*, 2021, **608**, 121037.
82 S. C. Karunakaran, B. J. Cafferty, K. S. Jain, G. B. Schuster and N. V. Hud, *ACS Omega*, 2020, **5**, 344–349.
83 H. Ren, Z. Zhang, X. Cheng, Z. Zou, X. Chen and C. He, *Sci. Adv.*, 2024, **10**, eadh4327.
84 X. Xue, K. Liang, W. Huang, H. Yang, L. Jiang, Q. Jiang, T. Jiang, B. Lin, Y. Chen, B. Jiang and S. Komarneni, *Macromolecules*, 2022, **55**, 6474–6486.
85 Z. Huang, X. Xiao, X. Jiang, S. Yang, C. Niu, Y. Yang, L. Yang, C. Li and L. Feng, *Polym. Test.*, 2023, **119**, 107936.
86 L. N. Woodard and M. A. Grunlan, *ACS Macro Lett.*, 2018, **7**, 976–982.
87 B. S. Alotaibi, A. K. Khan, M. Ijaz, H. Yasin, S. Nawazish, S. Sadiq, S. Kaleem and G. Murtaza, *ACS Omega*, 2023, **8**, 39014–39022.
88 Y. Li, Y. Yao, Y. Wang, Y. Lin, Y. He, S. Gao and X. Cai, *Nanoscale*, 2025, **17**, 15356–15365.
89 G. F. Hu, *Proc. Natl. Acad. Sci. U. S. A.*, 1998, **95**, 9791–9795.

90 P. Cuevas, D. Díaz-González and M. Dujovny, *Neurol. Res.*, 2003, **25**, 691–693.
91 P. Cuevas, D. Diaz-González, F. Carceller and M. Dujovny, *Neurol. Res.*, 2003, **25**, 13–16.
92 L. A. Tziveleka, A. Sapalidis, S. Kikionis, E. Aggelidou, E. Demiri, A. Kritis, E. Ioannou and V. Roussis, *Materials*, 2020, **13**, 1763.
93 O. S. Lawal, M. Yoshimura, R. Fukae and K. Nishinari, *Colloid Polym. Sci.*, 2011, **289**, 1261–1272.
94 S. C. Choi, M. A. Yoo, S. Y. Lee, H. J. Lee, D. H. Son, J. Jung, I. Noh and C. W. Kim, *J. Biomed. Mater. Res., Part A*, 2015, **103**, 3072–3080.
95 Y. Tan, Y. Zi, J. Peng, C. Shi, Y. Zheng and J. Zhong, *Food Chem.*, 2023, **423**, 136265.
96 K. J. Goudie, S. J. McCreath, J. A. Parkinson, C. M. Davidson and J. J. Liggat, *J. Polym. Sci.*, 2023, **61**, 2316–2332.
97 M. C. Koetting, J. T. Peters, S. D. Steichen and N. A. Peppas, *Mater. Sci. Eng., R*, 2015, **93**, 1.
98 G. Stojkov, Z. Niyazov, F. Picchioni and R. K. Bose, *Gels*, 2021, **7**, 255.
99 W. Zhang, L. Liu, H. Cheng, J. Zhu, X. Li, S. Ye and X. Li, *Mater. Adv.*, 2024, **5**, 1364–1394.
100 V. Dhote, S. Skaalure, U. Akalp, J. Roberts, S. J. Bryant and F. J. Vernerey, *J. Mech. Behav. Biomed. Mater.*, 2012, **19**, 61.
101 B. G. Stubbe, K. Braeckmans, F. Horkay, W. E. Hennink, S. C. De Smedt and J. Demeester, *Macromolecules*, 2002, **35**, 2501–2505.
102 Q. Xing, K. Yates, C. Vogt, Z. Qian, M. C. Frost and F. Zhao, *Sci. Rep.*, 2014, **4**, 1–10.
103 M. R. Bayat and M. Baghani, *J. Intell. Mater. Syst. Struct.*, 2021, **32**, 2349–2365.
104 A. B. Bello, D. Kim, D. Kim, H. Park and S. H. Lee, *Tissue Eng., Part B*, 2020, **26**, 164–180.
105 V. Tyagi and A. Thakur, *Results Mater.*, 2023, **20**, 100481.